BMC Pharmacology and Toxicology

RESEARCH

Open Access

Exploration of the optimal concentration of quercetin liposome nanoparticles for the treatment of liver damage

Nana Yin[1], Jian Pang[2] and Xiangyan Liu[3,4*]

Abstract

Background Hepatic injury is a common pathological process for a wide spectrum of liver diseases. Quercetin has been found to counteract this process by scavenging free radicals, but its therapeutic effect is limited due to poor water-solubility. Thus, the question of how to deliver quercetin to a target organ effectively with minimal side effects has remained a clinical challenge. Our previous research findings indicate that when quercetin is delivered in the form of liposomal nanoparticles, its targeting efficiency to the liver is significantly enhanced. Although quercetin liposomal nanoparticles have been shown to improve the therapeutic effect on liver damage compared to traditional quercetin treatment, the optimal dosage of liposomal quercetin still warrants further exploration. The aim of this study was therefore to ascertain whether there are differences in the therapeutic effects on liver damage at different dosages of quercetin liposomes and to determine the optimal dosage.

Methods 62 rats modeled with liver injury were enrolled and distributed into 4 groups, where they were treated with quercetin liposome nanoparticles, blank liposome nanoparticles, simple quercetin, and normal saline accordingly. Serum samples were measured for liver function indicators, and tissue samples were analyzed by pathohistological examination. Statistical analysis was performed to quantify the difference between the experimental and control groups.

Results Both liver function and histopathological examinations demonstrated enhanced therapeutic effects as the concentration of quercetin liposome drugs increased. Moreover, compared to traditional quercetin treatments, liposomal quercetin nanoparticles of varying concentrations uniformly provide better liver protection, with the highest dose group showing the best therapeutic effect. In addition, low concentration carrier liposome nanoparticles also showed a certain protective effect on the liver damage in rats.

Conclusion Liposomal quercetin nanoparticles exhibit superior efficacy in liver protection and repair compared to pure quercetin, with the highest dose group showing the best therapeutic effect.

Keywords Quercetin, Hepatic injury, Liposomal nanoparticles, Protective effect

*Correspondence:
Xiangyan Liu
liuxiangyan76@gmail.com
[1]Department of Operating Room, First People's Hospital of Changde, Changde, China
[2]Department of General Surgery, The Second Xiangya Hospital, Central South University, Changsha, China
[3]Department of Breast Surgery, Xiangya Hospital, Central South University, 87# Xiangya Road, Changsha City, Hunan Province 410008, PR China
[4]Clinical Research Center For Breast Cancer in Human Province, Changsha, China

Background

Hepatic injury is a common pathological process for a wide spectrum of liver diseases, such as viral hepatitis, fatty liver, alcoholic liver disease, drug induced liver disease, and toxic hepatopathy, that can lead to cirrhosis and fibrosis [1, 2]. Thus, the importance of early medical intervention cannot be overstated. In recent years, significant attention has been directed towards the relationship between free radicals and hepatic diseases, and researchers now widely accept that oxidative free radicals contribute to liver damage through the destruction of biological macromolecules, including hyaluronic acid, nucleic acids, and proteins [3, 4].

Quercetin, a distinct inhibitor of tyrosine protein kinase H1, demonstrates robust free radical neutralizing activity along with blood glucose regulatory effects [5, 6]. Its antioxidative attributes contribute to its therapeutic potential in managing diabetes, nephropathy, hepatic damage, and cardiac/cerebral ischemia-reperfusion injuries, and this potential is primarily realized by inhibiting nonenzymatic glycation, oxidative stress, and associated pathological processes [7]. However, due to its poor water solubility, the efficient delivery of quercetin to a target organ and the minimization of side effects both pose significant clinical challenges.

Drug delivery system that relies on nanotechnology, however, can amplify pharmacological bioavailability and expand therapeutic indications of many different medications [8, 9]. Liposomes in particular serve as an innovative targeted drug carrier since they enhance the therapeutic index of the drugs they can carry. By encapsulating a specific drug into nanoscale particles with cell-like structures, phagocytosis by the reticuloendothelial system can occur followed by immune system activation, allowing drugs to be redistributed to the liver, spleen, and bone marrow [10, 11].

Despite numerous studies indicating that quercetin and other flavonoids can protect the liver, the potential of quercetin liposome nanoparticles to enhance its protective function by increasing the drug concentration has been widely overlooked. Our prior research findings indicate that when quercetin is administered in the form of liposome nanoparticles, its targeting to the liver is markedly amplified [12]. Although quercetin liposome nanoparticles can enhance the therapeutic effect on liver damage compared to traditional quercetin treatment, the optimal dosage remains to be further investigated. The objective of this study was therefore to elucidate whether there is a variance in the therapeutic effect on liver damage at different dosages of quercetin liposomes and to ascertain the optimal therapeutic drug dosage.

Materials and methods

Instruments and reagents

The instruments utilized in this study included a transmission electron microscope (Hitachi, Japan), a laser particle size analyzer (Malvern Panalytical, UK), a 90Plus particle size analyzer (Brookhaven Instruments, USA), an optical microscope (Olympus, Japan), a TDL-5 centrifuge (JingHui, China), and a high-performance liquid chromatography (HPLC) system (Waters, USA). For HPLC analysis, mobile phase A was composed of a mixture of methanol, acetic acid, and phosphate buffer (pH 3.0; 34:6:60, v/v/v), and mobile phase B was comprised solely of acetonitrile. The gradient elution program was established as follows: 0 min (98% A:2% B), 0.1 min (80% A:20% B), 12 min (98% A:2% B), and 22 min (98% A:2% B) [13]. Experimental reagents used were as follows: Lipoid S100 (Batch No. 790495-1), procured from Lipoid GmbH (Germany), and quercetin (with a purity of ≥ 95% as established by HPLC), sourced from Sigma-Aldrich (Shanghai, China).

Preparation of Quercetin liposome nanoparticles

The preparation of quercetin liposome nanoparticles entailed a sequence of procedures, including their fabrication, encapsulation, and drug-loading.

(1) Fabrication: quercetin liposome nanoparticles were fabricated using the film dispersion-homogenization method [14]. In summary, quercetin-loaded liposomes were prepared using phosphatidylcholine, phosphatidylserine, and cholesterol in a molar ratio of 5:1:1 using an improved thin-film evaporation technique. The ethanol in the mixed solution was then removed through rotary evaporation at 37 °C, forming a thin solid film. Subsequently, the lipid film was hydrated with a 5% glucose solution at 37 °C through rotary hydration to produce a pale yellow suspension. Following ultrasonic treatment and high-pressure homogenization, the suspension was filtered through a 0.2 μm filter to remove unencapsulated drugs, thereby yielding the quercetin nanoliposomes [12]. The morphological attributes and particle size distribution were assessed using a laser particle size analyzer (Malvern Panalytical, UK), and their shape and size were further scrutinized using transmission electron microscopy (TEM, Hitachi, Japan) [15].

(2) Encapsulation and drug-loading: For the determination of encapsulation efficiency (EE) and drug-loading capacity, the nanoparticle suspensions were dissolved in methanol containing 10% Triton X-100, followed by HPLC analysis (Waters, USA). The dynamic dialysis technique was utilized to segregate the free drug, with drug concentrations quantified by HPLC. Encapsulation efficiency was

calculated as follows: EE% = (1−Wf/Wt) × 100%, where Wf denotes the amount of free drug in the system, and Wt represents the total amount of drug incorporated into the system [16].

Fabrication of blank liposome nanoparticles

The film dispersion-homogenizing method was employed for fabrication, using the same nanoparticle formulation as the experimental group, with the exception of the quercetin itself.

Animal ethics

All animal experimental procedures were approved by the Animal Ethics Committee of Xiangya Hospital, Central South University (Approval number: 201503239).

Establishment and grouping of animal models

(1) Animals: A total of 88 healthy Sprague Dawley (SD) rats (44 males and 44 females), initially weighing 80–120 g, were obtained from the Department of Laboratory Animals at Xiangya School of Medicine, Central South University. Each rat was housed individually in a cage with unrestricted access to food and tap water. The animals were maintained at a temperature of 25 ± 2 °C under a 12-hour dark/light cycle. At the end of the experiment, all animals were euthanized using sodium pentobarbital injection. Intraperitoneal injection was selected to minimize pain and discomfort. The dosage (150–200 mg/kg) was precisely calculated based on individual body weight to ensure rapid and painless loss of consciousness, followed by respiratory arrest. To uphold animal welfare and ethical standards, all procedures adhered to relevant ethical guidelines and regulatory protocols.

(2) Model Establishment: Hepatic injury was induced in 80 healthy SD rats via a modified combined method, and the remaining 8 rats served as the control group. Of the 80 rats, 18 fatalities occurred during the modeling process, for a mortality rate of 22.5%. Autopsies confirmed that the deaths were due to excessive anesthesia and carbon tetrachloride (CCl4) toxicity. Consequently, 62 rat models of hepatic injury were successfully established. The specific construction method is detailed as follows. Initially, a subcutaneous injection of CCl4 and castor oil mixture (CCl4:castor oil = 4:6) was administered at a dose of 0.5 mL/100 g of body weight. Subsequent injections of 0.3 mL/100 g were given every 3–4 days until all 13 doses were administered. The hepatic injury models were validated through pathological examination.

(3) Grouping: A total of 62 hepatic injury models were successfully established and randomly divided into five groups: Group A (18 rats, treated with quercetin liposome nanoparticles), Group B (18 rats, treated with quercetin), Group C (18 rats, treated with blank liposome nanoparticles), Group D (8 rats, injury control treated with normal saline), and Group E (8 healthy rats, normal control). Groups A, B, and C were further subdivided into high- (H), medium- (M), and low- (L) dosage subgroups (AH/AM/AL, BH/BM/BL, CH/CM/CL) to assess dosage effects.

(4) Feeding Protocol: During the experimental phase, all rats allocated to the treatment groups were subjected to a high-fat, corn-based diet, comprised of 79.5% corn flour, 10% lard, and 0.5% cholesterol, supplemented with 10% ethanol for an initial period of two weeks. This was then replaced with a regimen of pure corn flour and tap water for the following four weeks. In contrast, the control group was consistently provided with standard chow and tap water for the entirety of the study. Throughout this process, all animals were under regular surveillance, with daily records maintained regarding their physical status.

Treatment

As mentioned above, the experimental groups A, B, and C received intraperitoneal injections of quercetin liposome nanoparticles, free quercetin, and blank liposome nanoparticles, respectively. These groups were further subdivided into high-, medium-, and low-dose subgroups, each receiving dosages of 7.5 mg/100 g, 5 mg/100 g, and 2.5 mg/100 g, respectively. The control group and the injury control group received a daily dosage of 5 mg/100 g of normal saline for the first week, which then transitioned to an alternate-day injection regimen until a cumulative total of 20 doses were reached. Throughout the experiment, three rats died, including one from the BM group and two from group D. However, no fatalities were recorded among the 8 rats in group E. Autopsies confirmed that all deaths were liver-injury-related.

Tissue preparation

On the day after the final injection, 2 mL of blood was collected from the hepatic veins of each rat. Following euthanasia, liver tissue was harvested and divided into two portions: one was fixed in 4% formalin for pathological analysis, and the other was snap-frozen in liquid nitrogen and stored at − 80 °C for subsequent enzyme activity assay.

Measurement of liver function index

Prior to autopsy, blood was drawn from the vena cava and the resulting serum was subjected to a 37 °C water bath incubation for 30 min. This was followed by centrifugation at 2,500 rpm for 20 min, after which the supernatant was separated for subsequent analysis. Commercial kits were utilized to measure serum levels of aspartate aminotransferase (AST), alanine aminotransferase (ALT), total bile acid (TBA), and direct bilirubin (DBIL), in strict accordance with the manufacturer's guidelines. Liver tissues were preserved in 4% formalin for 24 h, processed into sections of 3 μm thickness, and subsequently stained with hematoxylin and eosin (H&E). Hepatic pathology was then assessed via light microscopy, and the proportion of normal cells was quantified utilizing ImageJ software.

Statistical methods

All variables of interest were expressed mean ± standard deviation prior to analysis. Statistical analysis of liver function indices was performed using analysis of variance, and histological examination results were analyzed using the chi-squared test. A P-value < 0.05 was considered to indicate statistically significant test results. All analyses were conducted using SPSS software (IBM Corp., Armonk, NY, USA).

Results

Characteristics of quercetin nanoliposomes

The quercetin nanoliposomes consisted of uniformly distributed spherical particles, with a size measuring 142 ± 19 nm and a drug load of 5.08 ± 0.17 mg/mL. They also exhibited a high entrapment efficiency of 90.2 ± 1.57%. Both the quercetin liposome nanoparticles and the blank liposome nanogranules formed uniform, stable solutions, with no observable stratification, opacities, or sedimentation, thus meeting the requirements for intravenous administration. The detailed characteristics of quercetin nanoliposomes have been reported in our previous study [12].

Liver function status at different drug concentrations

As illustrated in Table 1, serum levels of ALT, AST, TBA, and DBIL in the liver injury control group (Group D) were significantly elevated compared to the normal group (Group E) (all $P < 0.05$), thereby validating the successful establishment of the liver injury model. Furthermore, serum liver function markers in the nanoparticle drug groups with high, medium, and low dosages, the pure drug group, and the carrier group all showed improvement compared to the injury control group, suggesting a hepatoprotective effect. In both the conventional quercetin and liposomal quercetin treatment groups, an escalation in drug dosage also corresponded with a dose-dependent reduction in ALT, AST, TBA, and DBIL levels, indicating an enhanced recovery of liver function. Notably, the liposomal quercetin treatment group exhibited superior hepatoprotective effects across all dosage groups (high, medium, low) compared to the conventional quercetin group (all $P < 0.05$). Furthermore, as the concentration of liposomal quercetin nanoparticles increased, the liver function markers progressively improved, with significant differences in ALT and AST between the high- and low-dose groups (all $P < 0.05$). However, although the carrier group also demonstrated some protective effects against liver injury, this effect diminished with increasing carrier concentration. Only a mild hepatoprotective effect was observed at low carrier concentrations.

Pathological manifestations of the liver under different drug concentrations

In the control group (Group E), hepatocytes within the liver tissue were systematically arranged in strands, with each strand containing one or two spherical nuclei. The sinusoids were populated with blood cells, the hepatocyte cytoplasm demonstrated mild acidophilia, and the central vein typically presented a circular outline (Figure S1). In contrast, the liver histological sections stained with H&E from the injury control group (Group D) displayed significant hepatic fat accumulation, necrosis, inflammation, and fibrosis (Figure S2). Compared to group D, both

Table 1 Changes in serum ALT, AST, TBA, and DBIL

Group		ALT(u/L)	AST(u/L)	TBA (umol/L)	DBIL (umol/L)
Group A	High dose $n=6$	40.7 ± 3.56	75.2 ± 6.41	13.666 ± 3.345	0.266 ± 0.08
	Medium dose $n=6$	51.05 ± 6.3349	100.68 ± 4.137	14.916 ± 2.219	0.28 ± 0.075
	Low dose $n=6$	57.08 ± 4.787	105 ± 4.006	17.55 ± 3.6588	0.3 ± 0.089
Group B	High dose $n=6$	58.866 ± 10.32	102.68 ± 6.697	23.23 ± 4.119	0.53 ± 0.216
	Medium does $n=5$	66.86 ± 7.69	123.16 ± 9.147	24.24 ± 4.42	0.54 ± 0.207
	Low dose $n=6$	73.3 ± 6.5	128.±10.75	26.45 ± 2.98	0.56 ± 0.186
Group C	High dose $n=6$	262.6 ± 18.966	339 ± 32.177	93.2 ± 9.49	0.68 ± 0.18
	Medium dose $n=6$	164.35 ± 10.7	290.7 ± 5.7758	22.15 ± 4.018	0.5 ± 0.2449
	Low dose $n=6$	61.66 ± 14.98	153.85 ± 17.97	17 ± 5.999	0.366 ± 0.24
Group D	$n=6$	490.38 ± 18.9	779.85 ± 34.389	97.0666 ± 14	2.218 ± 0.276
Group E	$n=8$	30.766 ± 6.77	59.48 ± 12.248	9.48 ± 4.459	0.2 ± 0.1095

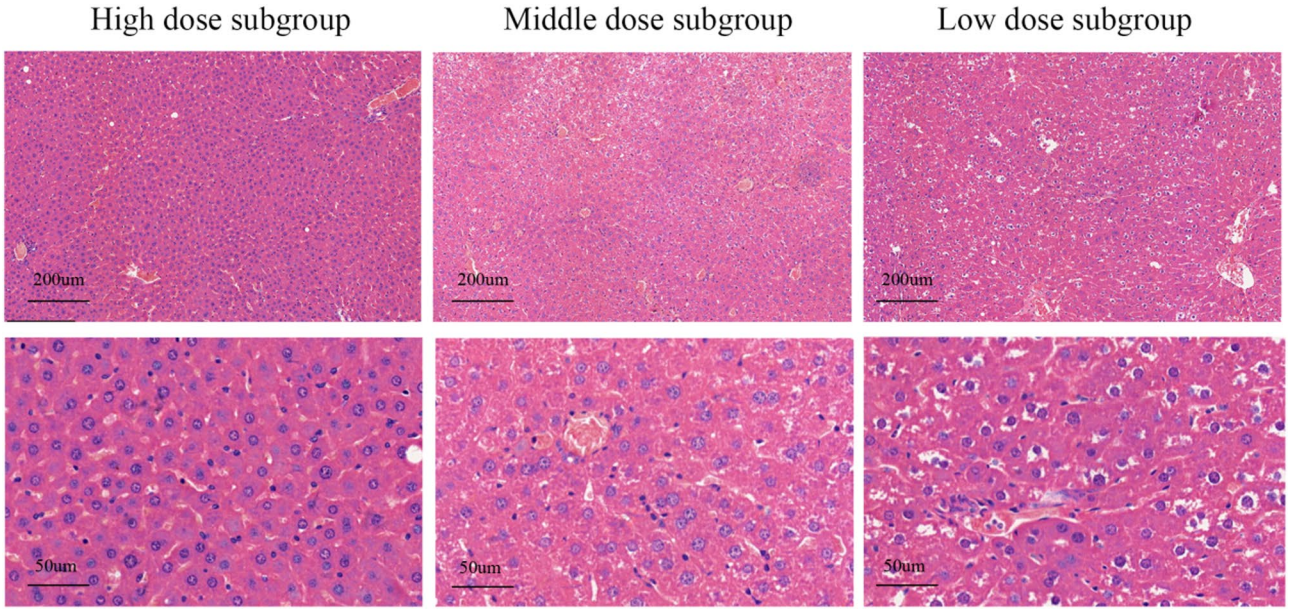

Fig. 1 The quercetin liposome nanoparticles groups: high dose subgroup; medium dose subgroup; low dose subgroup

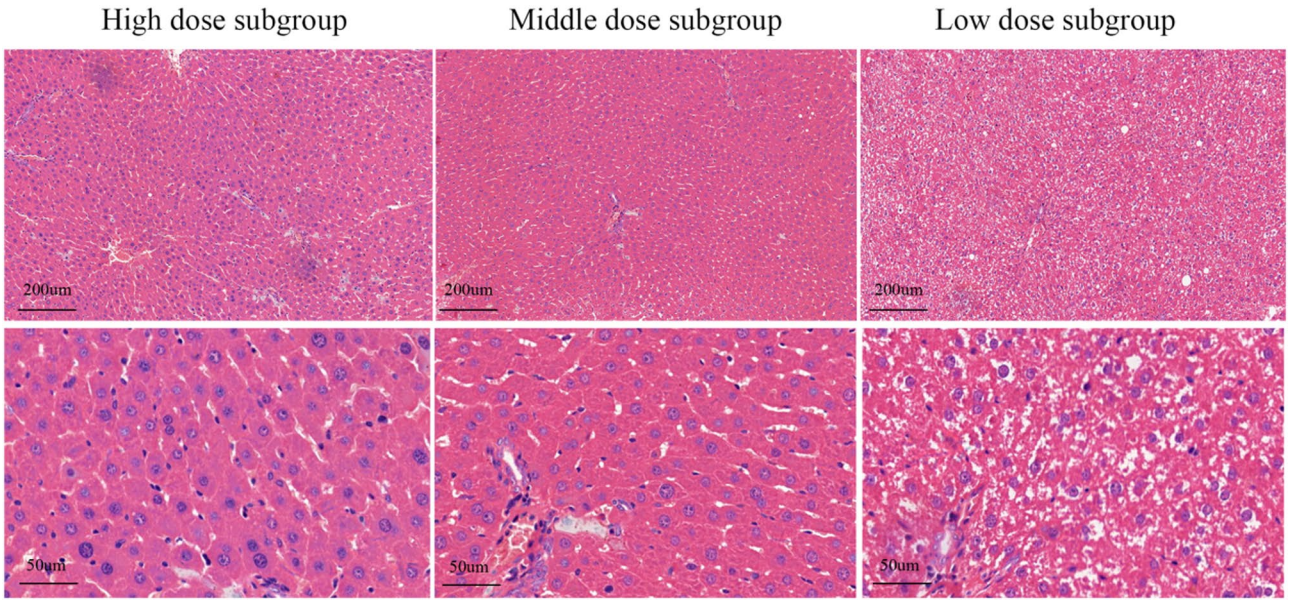

Fig. 2 The quercetin groups: high dose subgroup; medium dose subgroup; low dose subgroup

the quercetin liposome nanoparticle treatment group (Fig. 1: high-, medium-, and low-dose subgroups) and the quercetin treatment group (Fig. 2: high-, medium-, and low-dose subgroups) displayed dose-dependent improvements in terms of necrosis, inflammation, fat accumulation, and fibrosis. Within the liposome nanoparticle subgroups, the low-dose treatment (Fig. 3) did mitigate necrosis, inflammation, fat accumulation, and fibrosis, but the differences between the high- and medium-dose subgroups (Fig. 3) were less distinct. Additionally, the normal cell ratio was evaluated across all groups for each tissue section from every animal (Figure S3).

Discussion

Quercetin, which can be found in the flowers, leaves, and fruits of numerous plants, is a member of the flavonoid family and demonstrates a multitude of biological functions, such as antioxidant activity, free radical scavenging, and blood pressure- and lipid-lowering effects [17–19]. However, it cannot be administered intravenously due to its poor water solubility [20].

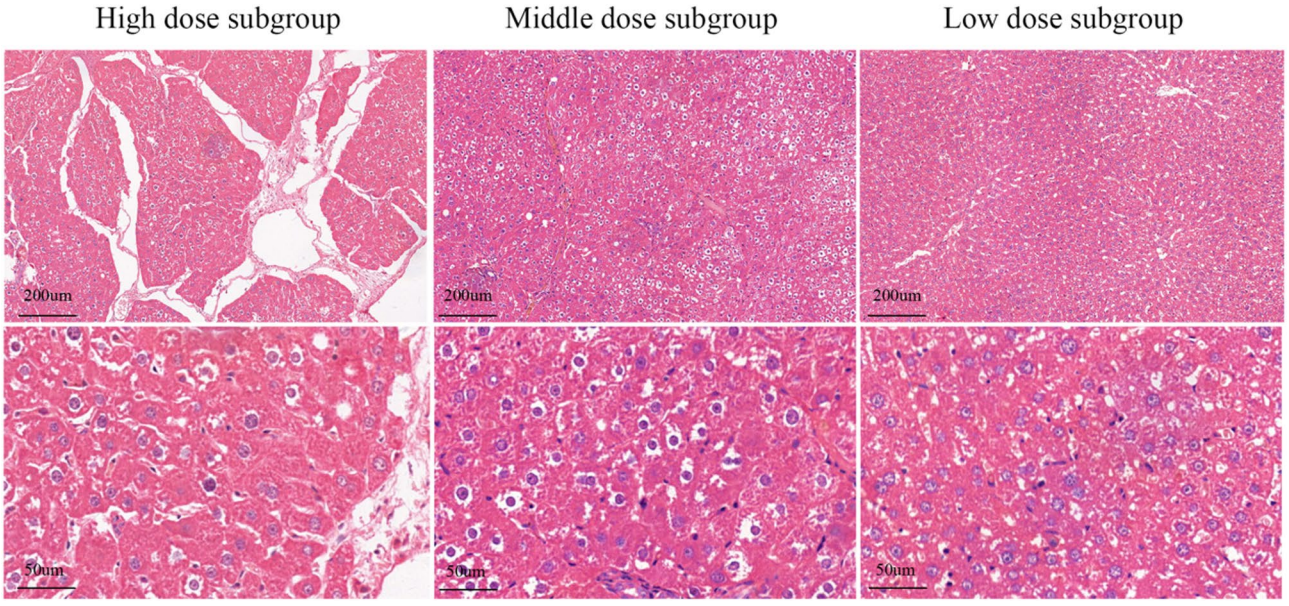

Fig. 3 The liposome nanometer-granules groups: high dose subgroup; medium dose subgroup; low dose subgroup

Nanomedicine represents an interdisciplinary field that integrates aspects of pharmaceutical engineering and nanotechnology. Due to their minuscule size, nanomedicines can readily permeate cell membranes, thereby augmenting intracellular drug accumulation [21]. Accordingly, compared to traditional therapies, lower drug doses can be employed to achieve superior therapeutic efficacy while simultaneously minimizing side effects. Liposomes, which are primarily composed of phospholipids that possess both hydrophilic and hydrophobic regions, present significant advantages over conventional drug carriers [12], including improved delivery of hydrophobic drugs, enhanced cellular uptake via endocytosis, prolonged therapeutic effects, and an elevated therapeutic index [22, 23]. The integration of liposomes with nanomedicine has already exhibited remarkable success in various applications.

A variety of factors can contribute to liver injury, among which CCl4-induced damage is the most commonly employed model for studying liver fibrosis [24]. CCl4 exerts potent oxidative stress on hepatocytes, leading to the dysfunction of subcellular organelles, including mitochondria [25]. The ensuing lesions play a pivotal role in fibrogenesis and, if left untreated, may progress to cirrhosis of the liver [26]. Typically, prolonged administration of CCl4 (over one month) induces liver injury and early-stage fibrosis [27]. In addition, chronic exposure to alcohol contributes to liver damage, as its metabolite, acetaldehyde, exacerbates glutathione depletion, lipid peroxidation, and mitochondrial dysfunction [28, 29]. In this study, liver injury was induced through a combination of subcutaneous CCl4 injections, a high-fat, high-cholesterol, low-protein diet, and 10% ethanol supplementation. The injury model was successfully established by the sixth week of the experiment.

Transaminases, such as AST and ALP, are released into the bloodstream as a result of hepatic lesions [30]. TBA is closely associated with liver metabolism, and researchers have established that the primary determinant of elevated TBA levels is impaired hepatic uptake, a common occurrence in patients with chronic liver diseases [31]. Elevated DBIL levels also suggest diminished hepatic uptake [32]. Except for TBA in the high-dose blank liposome nanoparticle group, the liver function indices (ALT, AST, and DBIL) in the injury control group were significantly elevated compared to those in all other groups. Histopathological examination was conducted to confirm the diagnosis due to the method's precision, and the results revealed disorganized hepatic lobules and cords, along with degeneration. Collagen and other extracellular matrix components accumulated around the portal area. Moreover, fibrosis formation, inflammatory cell infiltration, and steatosis were observed as well, and some hepatocytes displayed vacuolar degeneration and ballooning degeneration. Collectively, these findings indicated the successful establishment of the combined injury model.

As previously discussed, the liposome delivery system can inhibit rapid drug degradation, bolster stability, and extend drug release. Through passive targeting, it likewise enhances drug efficacy, escalates the therapeutic index at pathological sites, and plays a distinctive role in liver-specific drug delivery [33, 34]. Our findings revealed that an increasing dosage of quercetin liposomes resulted in a progressive decrease in serum AST and ALP levels in Group A. Moreover, significant downward trends were observed in comparison to Groups B and D across all

dosage categories (high, medium, and low). These observations imply that nanoparticles of quercetin liposomes not only exert hepatoprotective effects but also promote liver recovery, thereby showcasing enhanced therapeutic efficacy compared to treatment with unencapsulated quercetin.

We further noted that there was a progressive improvement in hepatological blood test indicators and that all four liver function markers in Group AH normalized with increasing concentration of liposomal quercetin nanoparticles. Histopathological examinations revealed that treatment with quercetin liposome nanoparticles assisted in preserving the cellular structure of hepatocytes, countering fibrosis and fatty degeneration, and promoting the repair of liver lobules. As the dosage of quercetin liposome nanoparticles increased, marked improvements were observed in liver cells, particularly in terms of reduced necrosis, inflammation, fat accumulation, and fibrosis. Furthermore, the liver structure of Group AH closely mirrored that of the blank control group, with no statistically significant differences in serum ALT, AST, TBA, and DBIL levels. The treatment was also confirmed to be safe in Group A rats, as no unexpected losses occurred during the experiment.

Interestingly, we also found no statistically significant differences in the serum ALT, AST, and DBIL levels between Group CL and Group BL, which suggests that blank liposome nanoparticles may also possess hepatoprotective potential. Histopathological examination revealed that the blank liposome nanoparticles may have aided in liver cell protection, with mild improvements seen in fatty degeneration, lobular necrosis, and hepatocyte degeneration. Notably, the therapeutic effect was more pronounced in the low-dose blank liposome nanoparticle treatment group compared to the medium- and high-dose liposome nanoparticles alone. In conclusion, blank liposome nanoparticles can facilitate the liver healing process, and the low-dose blank liposome nanoparticles appear to be the more beneficial option.

Indeed, this study does have certain limitations: Firstly, we did not delve into the specific mechanism of cellular uptake of nanoliposomes, which is a direction we are currently striving to explore. Secondly, the metabolic capability of rats towards quercetin liposome nanoparticles is also worth further investigation. Lastly, with the increase in drug dosage, monitoring common adverse reactions also holds significant research value.

Conclusion

Liposomal quercetin nanoparticles exhibit superior efficacy in liver protection and repair compared to pure quercetin, with the highest dose group showing the best therapeutic effect. This finding further confirms that the dosage of quercetin liposomes can impact the therapeutic effect on liver damage.

Supplementary Information

The online version contains supplementary material available at https://doi.org/10.1186/s40360-025-00951-x.

Supplementary Material 1

Acknowledgements
The authors thank AiMi Academic Services (www.aimieditor.com) for English language editing and review services.

Author contributions
N.N.Y.: Data compilation, writing—original draft and revision of the manuscript. J.P.: Data compilation, writing—original draft manuscript. X.Y.L.: Conceptualisation, funding acquisition, data curation, formal analysis, investigation, resources, supervision.The work reported in the article has been performed by the authors, unless clearly specified in the text. All authors reviewed the manuscript.

Funding
This project is funded by the Teaching Reform Project of Central South University (Project Number: 2021jy157).

Data availability
The data that support the findings of this study are available from the corresponding author, Xiangyan Liu, upon reasonable request.

Declarations

Ethical approval
This research was granted approval by the Animal Ethics Committee of Xiangya Hospital (Approval number: 201503239).

Consent for publication
Not applicable.

Competing interests
The authors declare no competing interests.

Received: 31 March 2024 / Accepted: 20 May 2025
Published online: 28 May 2025

References

1. Kim SM, et al. Hyaluronan synthase 2, a target of miR-200c, promotes carbon tetrachloride-induced acute and chronic liver inflammation via regulation of CCL3 and CCL4. Exp Mol Med. 2022;54:739–52. https://doi.org/10.1038/s12276-022-00781-5.
2. He H, et al. FBXO31 modulates activation of hepatic stellate cells and liver fibrogenesis by promoting ubiquitination of Smad7. J Cell Biochem. 2020;121:3711–9. https://doi.org/10.1002/jcb.29528.
3. Ančić M, et al. PHYSICO chemical properties and toxicological effect of landfill groundwaters and leachates. Chemosphere. 2020;238:124574. https://doi.org/10.1016/j.chemosphere.2019.124574.
4. Wang W, Jiang L, Ren Y, Shen M, Xie J. Characterizations and hepatoprotective effect of polysaccharides from mesona blumes against tetrachloride-induced acute liver injury in mice. Int J Biol Macromol. 2019;124:788–95. https://doi.org/10.1016/j.ijbiomac.2018.11.260.
5. Roy PK, Park SH, Song MG, Park SY. Antimicrobial efficacy of Quercetin against Vibrio parahaemolyticus biofilm on food surfaces and downregulation of virulence genes. Polym (Basel). 2022;14. https://doi.org/10.3390/polym14183847.
6. Khan MA, et al. Adsorption and recovery of polyphenolic flavonoids using TiO(2)-Functionalized mesoporous silica nanoparticles. ACS Appl Mater Interfaces. 2017;9:32114–25. https://doi.org/10.1021/acsami.7b09510.

7. Patel RV, et al. Therapeutic potential of Quercetin as a cardiovascular agent. Eur J Med Chem. 2018;155:889–904. https://doi.org/10.1016/j.ejmech.2018.06.053.
8. Ma X, Zhao Y, Liang XJ. Theranostic nanoparticles engineered for clinic and pharmaceutics. Acc Chem Res. 2011;44:1114–22. https://doi.org/10.1021/ar2000056.
9. Tang J, et al. Nanomaterials for delivering antibiotics in the therapy of pneumonia. Int J Mol Sci. 2022;23. https://doi.org/10.3390/ijms232415738.
10. Barenholz Y. Doxil®--the first FDA-approved nano-drug: lessons learned. J Control Release. 2012;160:117–34. https://doi.org/10.1016/j.jconrel.2012.03.020.
11. Wang J, et al. Pharmacokinetic parameters and tissue distribution of magnetic Fe(3)O(4) nanoparticles in mice. Int J Nanomed. 2010;5:861–6. https://doi.org/10.2147/ijn.S13662.
12. Liu X, et al. Protective and therapeutic effects of nanoliposomal Quercetin on acute liver injury in rats. BMC Pharmacol Toxicol. 2020;21. https://doi.org/10.1186/s40360-020-0388-5.
13. Yang KY, et al. Silymarin-loaded solid nanoparticles provide excellent hepatic protection: physicochemical characterization and in vivo evaluation. Int J Nanomed. 2013;8:3333–43. https://doi.org/10.2147/ijn.S50683.
14. Guo C, et al. A novel saponin liposomes based on the couplet medicines of Platycodon grandiflorum-Glycyrrhiza uralensis for targeting lung cancer. Drug Deliv. 2022;29:2743–50. https://doi.org/10.1080/10717544.2022.2112997.
15. Alnaief M, Obaidat RM, Alsmadi MM. Preparation of hybrid Alginate-Chitosan aerogel as potential carriers for pulmonary drug delivery. Polym (Basel). 2020;12. https://doi.org/10.3390/polym12102223.
16. Xu W, et al. Liver-Targeted nanoparticles facilitate the bioavailability and Anti-HBV efficacy of Baicalin in vitro and in vivo. Biomedicines. 2022;10. https://doi.org/10.3390/biomedicines10040900.
17. Kashyap D, et al. Fisetin and Quercetin: promising flavonoids with chemopreventive potential. Biomolecules. 2019;9. https://doi.org/10.3390/biom9050174.
18. Petrucci R, Bortolami M, Di Matteo P, Curulli A. Gold Nanomaterials-Based electrochemical sensors and biosensors for phenolic antioxidants detection: recent advances. Nanomaterials (Basel). 2022;12. https://doi.org/10.3390/nano12060959.
19. Munot N et al. A Comparative Study of Quercetin-Loaded Nanocochleates and Liposomes: Formulation, Characterization, Assessment of Degradation and In Vitro Anticancer Potential. *Pharmaceutics* 14. https://doi.org/10.3390/pharmaceutics14081601 (2022).
20. Uchiyama H, et al. Single-stranded β-1,3– 1,6-glucan as a carrier for improved dissolution and membrane permeation of poorly water-soluble compounds. Carbohydr Polym. 2020;247:116698. https://doi.org/10.1016/j.carbpol.2020.116698.
21. Abdelwahab M, Salahuddin N, Gaber M, Mousa M. Poly(3-hydroxybutyrate)/polyethylene glycol-NiO nanocomposite for NOR delivery: antibacterial activity and cytotoxic effect against cancer cell lines. Int J Biol Macromol. 2018;114:717–27. https://doi.org/10.1016/j.ijbiomac.2018.03.050.
22. Diaz-Palomera CD, et al. Topical Pirfenidone-Loaded liposomes ophthalmic formulation reduces haze development after corneal alkali burn in mice. Pharmaceutics. 2022;14. https://doi.org/10.3390/pharmaceutics14020316.
23. Roberts SA, Lee C, Singh S, Agrawal N. Versatile encapsulation and synthesis of potent liposomes by thermal equilibration. Membr (Basel). 2022;12. https://doi.org/10.3390/membranes12030319.
24. Lin Y, et al. HGF/R-spondin1 rescues liver dysfunction through the induction of Lgr5(+) liver stem cells. Nat Commun. 2017;8:1175. https://doi.org/10.1038/s41467-017-01341-6.
25. Abu-Rizq HA, Mansour MH, Safer AM, Afzal M. Cyto-protective and Immunomodulating effect of Curcuma longa in Wistar rats subjected to carbon tetrachloride-induced oxidative stress. Inflammopharmacology. 2008;16:87–95. https://doi.org/10.1007/s10787-007-1621-1.
26. Galicia-Moreno M, et al. N-acetylcysteine prevents carbon tetrachloride-induced liver cirrhosis: role of liver transforming growth factor-beta and oxidative stress. Eur J Gastroenterol Hepatol. 2009;21:908–14. https://doi.org/10.1097/MEG.0b013e32831f1f3a.
27. Gong Z, et al. Genome–wide identification of long noncoding RNAs in CCl4–induced liver fibrosis via RNA sequencing. Mol Med Rep. 2018;18:299–307. https://doi.org/10.3892/mmr.2018.8986.
28. Cho YE, Yu LR, Abdelmegeed MA, Yoo SH, Song BJ. Apoptosis of enterocytes and nitration of junctional complex proteins promote alcohol-induced gut leakiness and liver injury. J Hepatol. 2018;69:142–53. https://doi.org/10.1016/j.jhep.2018.02.005.
29. Ganne-Carrié N, Nahon P. Hepatocellular carcinoma in the setting of alcohol-related liver disease. J Hepatol. 2019;70:284–93. https://doi.org/10.1016/j.jhep.2018.10.008.
30. Long X, et al. Preventive effect of Limosilactobacillus fermentum SCHY34 on lead Acetate-Induced neurological damage in SD rats. Front Nutr. 2022;9:852012. https://doi.org/10.3389/fnut.2022.852012.
31. Qi Y, et al. Zinc supplementation alleviates lipid and glucose metabolic disorders induced by a High-Fat diet. J Agric Food Chem. 2020;68:5189–200. https://doi.org/10.1021/acs.jafc.0c01103.
32. Mohsin MA, et al. Differentiation of subclinical ketosis and liver function test indices in adipose tissues associated with hyperketonemia in postpartum dairy cattle. Front Vet Sci. 2021;8:796494. https://doi.org/10.3389/fvets.2021.796494.
33. Pinto AM, Silva MD, Pastrana LM, Bañobre-López M, Sillankorva S. The clinical path to deliver encapsulated phages and lysins. FEMS Microbiol Rev. 2021;45. https://doi.org/10.1093/femsre/fuab019.
34. Yu J, et al. Remote loading paclitaxel-doxorubicin prodrug into liposomes for cancer combination therapy. Acta Pharm Sin B. 2020;10:1730–40. https://doi.org/10.1016/j.apsb.2020.04.011.

Publisher's note